Heat Mass Transfer (2009) 46:83–94
DOI 10.1007/s00231-009-0546-1

ORIGINAL

Exact solution of conductive heat transfer in cylindrical composite laminate

M. H. Kayhani · M. Shariati · M. Nourozi · M. Karimi Demneh

Received: 14 October 2008 / Accepted: 23 September 2009 / Published online: 9 October 2009

Abstract This paper presents an exact solution for steady-state conduction heat transfer in cylindrical composite laminates. This laminate is cylindrical shape and in each lamina, fibers have been wound around the cylinder. In this article heat transfer in composite laminates is being investigated, by using separation of variables method and an analytical relation for temperature distribution in these laminates has been obtained under specific boundary conditions. Also Fourier coefficients in each layer obtain by solving set of equations that related to thermal boundary layer conditions at inside and outside of the cylinder also thermal continuity and heat flux continuity between each layer is considered. In this research *LU* factorization method has been used to solve the set of equations.

1 Introduction

Today, using composite materials for manufacturing equipment, machinery and structures has been remarkably developed. By using these materials, the weight of equipment and structures is reduced (the mechanical strength remains constant) also the expense will be decreased by using these materials. In some industries, utilizing of these materials is unique compare to isotropic materials. Scientific works usually focus on the behavior of such materials under mechanical and thermal loads and rarely have observed other effects like heat transfer in these categories of materials. One of the most important applications of heat conduction in composite materials is manufacturing process which includes curing, cutting, fiber placement welding, etc. Some works have already been done on heat transfer in anisotropic materials. Early work in this era is based on 1-dimensional heat transfer in anisotropic crystals [1, 2]. Solutions of heat conduction in cylindrical coordinate have been obtained for homogeneous media with isotropy or special anisotropy [3–6].

Mulholland [7] researched on unsteady diffusion phenomena within an orthotropic cylinder and it was one of the preliminary works in this case. Noor and Burton [8] studied steady-state heat conduction in multilayered composite plates and shells. Extensive numerical results are presented for linear steady-state heat conduction problems, showing the effects of variation in the geometric and lamination parameters on the accuracy of the thermal response predictions of the predictor–corrector approach. Both antisymmetrically laminated anisotropic plates and multilayered orthotropic cylinders are considered. Vinayak and Iyengar [9] studied transient thermal conduction in rectangular fiber reinforced composite laminates. They used a finite element formulation based on the Fourier law of heat conduction to analyze the transient temperature distribution in rectangular fiber reinforced composite plates. For their studies, Results presented for graphite/epoxy and graphite–graphite/epoxy plates subjected to different thermal boundary conditions. Laminate with fiber orientations of 0°, ±45°, and 90° are considered for the analysis. Argyris et al. [10] presented theoretical formulation and computation of a three node six degree of freedom multilayer flat triangular element intended for the study of the temperature field in complex multilayer composite shells. This formulation consists of three modes of heat transfer: conduction,

M. H. Kayhani · M. Shariati · M. Nourozi
Department of Mechanical Engineering,
Shahrood University of Technology, Shahrood, Iran

M. Karimi Demneh (✉)
Department of Mechanical Engineering,
Sama College, Karaj Azad University, Karaj, Iran
e-mail: morius2000@yahoo.com

convection and radiation. In this article the formulation is based on a first-order thermal lamination theory which assumes a linear temperature variation along the thickness. They showed that this method is highly efficient compare to other numerical methods. Sugimoto et al. [11] represented a numerical analysis of heat conduction in multi-lamina plates also they studied effect of heat conduction from inner layers induced by the thermoplastic effect. Tarn and Wang [12–15] studied the heat conduction in circular cylinder of functionally graded materials (FGM) and laminated composites. Golovchan and Artemenko [16] solved the problem of the heat flux in a medium with orthogonally positioned rows of periodically applied fibers. Shi-qiang and Jia-chan [17] used two-space method, homogenized equation for steady heat conduction in the composite material cylinders. They showed the microscopic heat conduction in anisotropic when the cross-sections of the impurity cylinders are unidirectional oriented and isotropic when the angular distribution of the cross-sections is uniform.

Guo et al. [18] investigated development of temperature distribution of thick polymeric matrix laminates and compared it with numerically calculated results. The finite element formulation of the transient heat transfer problem was carried out for polymeric matrix composite materials from the heat transfer differential equations including internal heat generation produced by exothermic chemical reactions. Greengard and Lee [19] presented a robust integral equation method for the calculation of the electro static and properties of high contrast composite materials. Lu et al. [20] obtained analytical solution of transient heat conduction in composite circular cylinder slab (each layer is isotropic). They used the separation of variables method and showed that this form of solution has a good agreement with numerical results. Chatterjee et al. [21] presented an efficient boundary element formulation for 3-dimensional steady-state heat conduction analysis of fiber reinforced composites. The variations in the temperature and flux fields in the circumferential direction of the fiber are represented in terms of a trigonometric shape function together with a linear or quadratic variation in the longitudinal direction. Yvonnet et al. [22] established suitable formulation for the numerical computation of the effective thermal conductivities of a particulate composite in which the inclusions have different sizes and arbitrary shapes and the interfaces are highly conducting. An extended finite element method (XFEM) has been used in tandem with a level-set technique to elaborate an efficient numerical procedure for modeling highly conducting curved interfaces without resort to curvilinear coordinates and surface elements. Sadowski et al. [23] analyzed a sudden cooling process (thermal shock) at the upper side of FGM circular plates having discrete variation of the composite features. The non-stationary heat conduction equation was solved for arbitrary smooth or step variation of functions describing properties of the analyzed material. Chiu et al. [24, 25] used the thermal-electrical analogy [24] and parameter estimation technique [25] to calculating the effective thermal conductivity coefficients of spiral woven composite laminates. In addition to calculating the thermal properties of these laminates, they solved direct and inverse problem of conductive heat transfer using the alternating direction implicit (ADI) method and Levenberg–Marquardt algorithm, respectively. In this paper 2-dimensional steady-state heat transfer in a composite cylinder has been investigated and an exact analytical solution for the temperature distribution has been achieved for a cylinder subject with constant temperature on inside and sun radiation and natural convection at the same time from outside. In this research, separation of variables method has been used to solve the heat transfer equation and the Fourier coefficients were obtained by boundary conditions and continuity equations for temperature and heat flux between layers. To the best knowledge of authors, there is no any exact analytical investigation about heat conduction in cylindrical composite laminates. Research of Chiu et al. [25] is one of the similar works which using the ADI method (as a numerical method) to solving the direct problem in spiral woven composites with different kinds of boundary conditions. In these laminates, each lamina is made as a spiral round disc while in current research, the shape of lamina is as a cylindrical shell. The solution which presented in current research has an application in thermal studies of composite pipes, vessels and reservoirs. From thermal point of view, the results taken from exact solution can be used in thermal stress and strain analysis. In this work, theory of conductive heat transfer has been elaborated as well and the method for determining the heat transfer coefficients out of matrix material and fibers' properties are fully explained.

2 Heat conduction in composites

Generally, Fourier relation for conductive heat transfer in orthotropic materials is as below [3]:

$$\begin{Bmatrix} q_x \\ q_y \\ q_z \end{Bmatrix} = - \begin{bmatrix} k_{11} & k_{12} & k_{13} \\ k_{21} & k_{22} & k_{23} \\ k_{31} & k_{32} & k_{33} \end{bmatrix} \begin{Bmatrix} \frac{\partial T}{\partial x} \\ \frac{\partial T}{\partial y} \\ \frac{\partial T}{\partial z} \end{Bmatrix}. \quad (1)$$

According to the Onsager reciprocity, the tensor of conductive heat transfer coefficients should be symmetric. That is, for all substances in nature, we should have:

$$k_{ij} = k_{ji}. \quad (2)$$

Also according to the second law of thermodynamics, the diametric elements of this tensor are positive and the following equation must be valid [3]:

$$k_{ii}k_{jj} > k_{ij}^2 \quad \text{for}: i \neq j. \tag{3}$$

According to the Clausius–Duhem relation, the following inequalities are governed between coefficients of the conductivity tensor of orthotropic materials [3, 26, 27]:

$$k_{(ii)} \geq 0, \tag{4a}$$

$$\frac{1}{2}\left(k_{(ii)}k_{(jj)} - k_{(ij)}k_{(ji)}\right) \geq 0, \tag{4b}$$

$$\varepsilon_{ijk}k_{(1j)}k_{(2j)}k_{(3j)} \geq 0, \tag{4c}$$

where, $k_{(ij)}$ introduces symmetric part of conductivity tensor:

$$k_{(ij)} \equiv k_{(ij)} = \frac{k_{ij} + k_{ji}}{2}. \tag{5}$$

In general, two different coordinate systems are defined: on-axis (x_1, x_2, x_3) and off-axis (x, y, z) [28]. As shown in Fig. 1, the direction of on-axis coordinates depends on fiber orientation, in a way that x_1 is in direction of the fibers, x_2 is perpendicular to x_1 in the composite layers and x_3 is perpendicular to the layer plane. In manufacturing the composite materials, by laying the different layers on each other, the composite laminate is formed. Since the orientation of fibers in each lamina may be differed from other laminas. We need to define an off-axis reference coordinate system as well, so as to be able to study the physical properties in constant directions. Thus, there is an angular deviation by θ between the on-axis and off-axis system and these coordinates are coincident. In the on-axis coordinate system, Fourier equation for a composite material is [29]:

$$\begin{Bmatrix} q_1 \\ q_2 \\ q_3 \end{Bmatrix}_{\text{on}} = -\begin{bmatrix} k_{11} & 0 & 0 \\ 0 & k_{22} & 0 \\ 0 & 0 & k_{22} \end{bmatrix}_{\text{on}} \begin{Bmatrix} \frac{\partial T}{\partial x_1} \\ \frac{\partial T}{\partial x_2} \\ \frac{\partial T}{\partial x_3} \end{Bmatrix}_{\text{on}}. \tag{6}$$

According to Eq. 6, in each lamina; properties in direction of fibers (x_1) is different from those in perpendicular directions (x_2, x_3), but in the perpendicular plane to the fibers, heat transfer in all directions is the same. With rotation of on-axis system by $-\theta$, Eq. 6 can be obtained in the off-axis system:

$$[T(-\theta)]\{q\}_{\text{off}} = -[k]_{\text{on}}[T(-\theta)]\nabla T_{\text{off}}. \tag{7}$$

In Eq. 7, $T(\theta)$ is the rotation tensor transform and is derived from the following relation:

$$[T(\theta)] = \begin{bmatrix} \cos\theta & -\sin\theta & 0 \\ \sin\theta & \cos\theta & 0 \\ 0 & 0 & 1 \end{bmatrix}. \tag{8}$$

By using Eq. 7, the heat flux in off-axis directions is achieved as follow:

$$\{q\}_{\text{off}} = -[T(-\theta)]^{-1}[k]_{\text{on}}[T(-\theta)]\nabla T_{\text{off}}. \tag{9}$$

Since the rotation transform tensor is orthogonal, so:

$$[T(\theta)]^{-1} = [T(-\theta)]. \tag{10}$$

By substituting from Eq. 10 into Eq. 9, the heat flux vector in off-axis directions will be as follows:

$$\{q\}_{\text{off}} = -[T(\theta)][k]_{\text{on}}[T(-\theta)]\nabla T_{\text{off}}. \tag{11}$$

According to Fourier law, heat flux in off-axis directions is:

$$\{q\}_{\text{off}} = -[k]_{\text{off}}\nabla T_{\text{off}}. \tag{12}$$

Thus by comparing Eqs. 11 and 12, off-axis heat transfer coefficients tensor in terms of on-axis coordinate system is given below:

$$[k]_{\text{off}} = [T(\theta)][k]_{\text{on}}[T(-\theta)]. \tag{13}$$

The heat transfer coefficients tensor in on-axis system and off-axis system are shown by $[k]$ and $[\bar{k}]$, respectively, and cos θ is shown by m_1 and sinθ by n_1, Eqs. 6, 8 and 13 can be used to obtain the tensor elements of heat transfer coefficients in off-axis directions:

$$\begin{aligned} \bar{k}_{11} &= m_l^2 k_{11} + n_l^2 k_{22} \\ \bar{k}_{22} &= n_l^2 k_{11} + m_l^2 k_{22} \\ \bar{k}_{33} &= k_{22} \\ \bar{k}_{12} &= \bar{k}_{21} = m_l n_l (k_{11} - k_{22}) \\ \bar{k}_{13} &= \bar{k}_{31} = 0 \\ \bar{k}_{23} &= \bar{k}_{32} = 0 \end{aligned} \tag{14}$$

Now, the conductive coefficients in on-axis system (k_{11}, k_{22}) can be determined. Generally, two methods are suggested to calculate the conduction coefficients in on-axis system:

1. Doing a test to specify conduction coefficients on a lamina in the fibers direction and the perpendicular direction of them.
2. Using a certain formulation based on conductive coefficients of the fibers, matrix and volume percentage of the fibers [29].

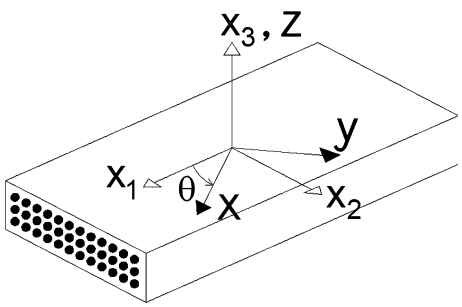

Fig. 1 On axis and off-axis coordinate systems

The second method is a suitable method that it is useful when there is lack of the appropriate laboratory equipment can be so helpful specifically when (especially in engineering calculations). In this method, heat transfer coefficients (or other directional dependent physical parameters of the substance) are calculable based on the following relations [29]:

$$k_{11} = v_f k_f + v_m k_m \tag{15a}$$

$$k_{22} = k_m \frac{1 + \zeta \eta v_f}{1 - \eta v_f} \tag{15b}$$

Quantities ζ and η are also calculated from the following equations:

$$\eta = \frac{k_f/k_m - 1}{k_f/k_m + \zeta} \tag{16a}$$

$$\zeta = 1/(4 - 3v_m) \tag{16b}$$

In general, Eqs. 15a, b and 16a, b can be generalized to other physical properties of the composite materials. For instance by using these relations many quantities such as dielectric constant, magnetic permeability, electrical conduction coefficient and diffusion coefficient for composites can be obtained [29].

3 Modeling and formulations

In this research, steady-state heat transfer in a composite cylinder has studied. According to Fig. 2, the fibers in each layer have been wounded in specific directions around the cylinder. The Fourier relation in cylindrical coordinate system for orthotropic material is given below:

$$\begin{Bmatrix} q_r \\ q_\varphi \\ q_z \end{Bmatrix} = - \begin{bmatrix} \bar{k}_{11} & \bar{k}_{12} & \bar{k}_{13} \\ \bar{k}_{21} & \bar{k}_{22} & \bar{k}_{23} \\ \bar{k}_{31} & \bar{k}_{32} & \bar{k}_{33} \end{bmatrix} \begin{Bmatrix} \frac{\partial T}{\partial r} \\ \frac{1}{r}\frac{\partial T}{\partial \varphi} \\ \frac{\partial T}{\partial z} \end{Bmatrix}. \tag{17}$$

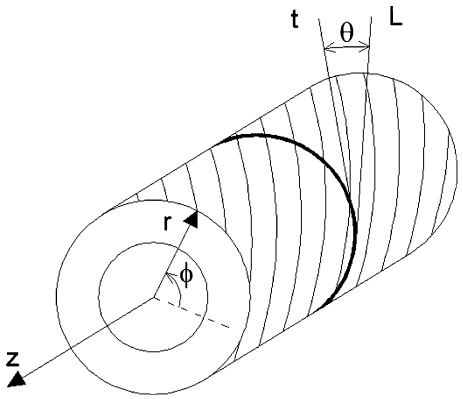

Fig. 2 The fibers' direction in a cylindrical laminate

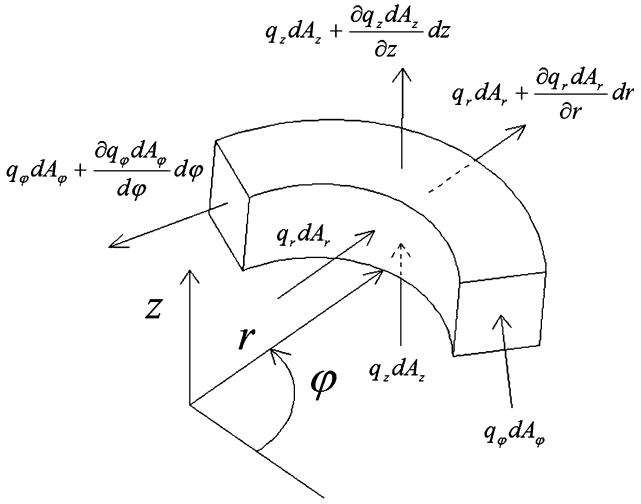

Fig. 3 Heat fluxes in a cylindrical element

So with applying the balance of energy in element of cylinder that has shown in Fig. 3, the following relation is obtained:

$$\rho C \frac{\partial T}{\partial t} dV = -\frac{\partial q_r dA_r}{\partial r} dr - \frac{\partial q_\varphi dA_\varphi}{\partial \varphi} d\varphi - \frac{\partial q_z dA_z}{dz} dz. \tag{18}$$

Relations for surfaces and volume of the cylindrical element are as below:

$$dA_r = r d\varphi dz, \tag{19a}$$

$$dA_\varphi = dr dz, \tag{19b}$$

$$dA_z = r d\varphi dr, \tag{19c}$$

$$dV = r d\varphi dr dz. \tag{19d}$$

Relation (17) and (19a–d) act on relation (18), then below relation will acquire for heat transfer in an orthotropic material [30, 31]:

$$\bar{k}_{11} \frac{1}{r} \frac{\partial}{\partial r} \left(r \frac{\partial T}{\partial r} \right) + \bar{k}_{22} \frac{1}{r^2} \frac{\partial^2 T}{\partial \varphi^2} + \bar{k}_{33} \frac{\partial^2 T}{\partial z^2} + (\bar{k}_{12} + \bar{k}_{21}) \frac{1}{r} \frac{\partial^2 T}{\partial \varphi \partial r} + (\bar{k}_{13} + \bar{k}_{31}) \frac{\partial^2 T}{\partial r \partial z} + \frac{k_{13}}{r} \frac{\partial T}{\partial z} + (\bar{k}_{23} + \bar{k}_{32}) \frac{1}{r} \frac{\partial^2 T}{\partial \varphi \partial z} = \rho C \frac{\partial T}{\partial t}. \tag{20}$$

In order to second law of thermodynamics, the coefficients of Eq. 20 must be remain in elliptic form for each 2-dimensional situation. Also unlike the isotropic materials, in orthotropic materials, the heat transfer in steady-state condition depends on properties of material.

Heat transfer equation for a cylindrical composite laminate can be determined from relation (20). In order to Fig. 2 it is obvious that the fibers angle was defined compare to φ axis and φ is a second orientation of coordinate system r, φ and z. Therefore, heat conductive coefficients must be rearranged [because in the relation (14), the fibers angle has been defined compare to first orientation of

coordinate system]. The rearranged relation (14) for a cylindrical lamina is given below:

$$\begin{aligned}
\bar{k}_{11} &= k_{22} \\
\bar{k}_{22} &= m_l^2 k_{11} + n_l^2 k_{22} \\
\bar{k}_{33} &= n_l^2 k_{11} + m_l^2 k_{22} \\
\bar{k}_{12} &= \bar{k}_{21} = 0 \\
\bar{k}_{13} &= \bar{k}_{31} = 0 \\
\bar{k}_{23} &= \bar{k}_{32} = m_l n_l (k_{11} - k_{22})
\end{aligned} \tag{21}$$

with substituting Relation (21) on relation (20), the heat transfer equation in this cylindrical laminate were acquired:

$$k_{22}\frac{1}{r}\frac{\partial}{\partial r}\left(r\frac{\partial T}{\partial r}\right) + \left(m_l^2 k_{11} + n_l^2 k_{22}\right)\frac{1}{r^2}\frac{\partial^2 T}{\partial \varphi^2} + \left(n_l^2 k_{11} + m_l^2 k_{22}\right)\frac{\partial^2 T}{\partial z^2} + 2m_l n_l (k_{11} - k_{22})\frac{1}{r}\frac{\partial^2 T}{\partial \varphi \partial z} = \rho C\frac{\partial T}{\partial t} \tag{22}$$

In steady-state condition, the right-hand side of Eq. 22 is zero. For a two phase fluid flows in a tube, we can suppose that temperature is constant inside the tube and if boundary condition at outside of the cylinder is not function of z, temperature gradient in long tube will be zero in z direction [31]. In this paper, these conditions were considered for cylinder. Therefore, Eq. 22 will simplify by using these conditions:

$$k_{22}\frac{1}{r}\frac{\partial}{\partial r}\left(r\frac{\partial T}{\partial r}\right) + \left(m_l^2 k_{11} + n_l^2 k_{22}\right)\frac{1}{r^2}\frac{\partial^2 T}{\partial \varphi^2} = 0. \tag{23}$$

In outside of cylinder, the convection and solar radiation are supposed for boundary conditions:

$$-k_{22}\frac{\partial T}{\partial r} = -q''(\varphi) + h(T - T_\infty). \tag{24}$$

Solar radiation flux and can be calculated from below relation [31]:

$$q''(\varphi) = \begin{cases} q'' \sin\varphi & 0 \le \varphi \le \pi \\ 0 & \pi < \varphi < 2\pi \end{cases}. \tag{25}$$

It is important to note that, these boundary conditions were optional choices and other boundary conditions can be implemented easily by using presented method in this article.

A cylindrical laminate could be made of multi layers and orientation of fibers in each layer may be different from others, so Eq. 23 will be different in each layer and temperature continuity and heat flux continuity must be implemented between each two layers. In Fig. 4 layers in cylindrical lamina have been shown. Therefore, if $r = r_i$ and there is boundary between two layers i and $i + 1$, so in this radius:

$$T^{(i)} = T^{(i+1)}, \tag{26a}$$

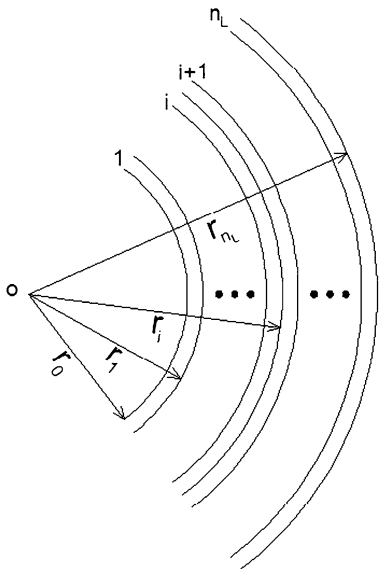

Fig. 4 Arrangement of layers in a cylindrical laminate

$$-k_{22}\frac{\partial T^{(i)}}{\partial r} = -k_{22}\frac{\partial T^{(i+1)}}{\partial r}. \tag{26b}$$

4 Analytical solution of heat conduction in a cylindrical laminate

In this section, analytical solution is given for equation of conductive heat transfer in composite laminate [relation (23)]. At the first, it is necessary to rewrite Eq. 23 as following formulation:

$$\frac{\partial^2 T}{\partial r^2} + \frac{1}{r}\frac{\partial T}{\partial r} + \frac{1}{\mu^2 r^2}\frac{\partial^2 T}{\partial \varphi^2} = 0. \tag{27}$$

In above relation, μ is:

$$\mu = \sqrt{\frac{k_{22}}{m_l^2 k_{11} + n_l^2 k_{22}}}. \tag{28}$$

In especial conditions, if angle of fibers (φ) equals to 90°, then $m_1 = 0$ and $n_1 = 1$. In this condition, $\mu = 1$ and relation (27) is similar to 2-dimensional heat transfer equation in isotropic materials. In this paper for solving Eq. 27 we had used separation of variables method. According to this method, heat distribution in two dimension, r and φ able to separate in two functions; $F(r)$ and $G(\varphi)$:

$$T(r, \varphi) = F(r)G(\varphi). \tag{29}$$

With acting Relation (29) on relation (27), heat transfer equation separates to two below equations:

$$r^2 F'' + rF' - \lambda_n^2 F = 0, \tag{30a}$$

$$G'' + \mu^2 \lambda_n^2 G = 0. \tag{30b}$$

In Eq. 30a, b, parameter λ_n is eigenvalue for heat transfer equation. λ_n determines from acting boundary condition on Eq. 30b.

This laminate is an annular shape. Therefore, temperature and its derivation continuity conditions must be satisfied:

$$G(0) = G(2\pi), \tag{31a}$$

$$G'(0) = G'(2\pi). \tag{31b}$$

General answer for this equation is given below:

$$G(\varphi) = A_n \cos(\mu\lambda_n\varphi) + B_n \sin(\mu\lambda_n\varphi). \tag{32}$$

By substituting relation (32) on boundary conditions [relation (31a, b)], below equations are obtained:

$$\begin{cases} A_n(\cos(2\pi\mu\lambda_n) - 1) + B_n \sin(2\pi\mu\lambda_n) = 0 \\ A_n \sin(2\pi\mu\lambda_n) - B_n(\cos(2\pi\mu\lambda_n) - 1) = 0 \end{cases}. \tag{33}$$

These equations are homogeneous; therefore their answers are zero unless they are linear dependent. In other word if determinant of coefficients in Eq. 33 is zero then answers are available.

$$(\cos(2\pi\mu\lambda_n) - 1)^2 + \sin^2(2\pi\mu\lambda_n) = 0. \tag{34}$$

By solving trigonometric equation (34), eigenvalues for heat transfer equation in each layer are given:

$$\lambda_n = \frac{n}{\mu} \quad n = 0, 1, 2, \ldots \tag{35}$$

Equation 30a is Cauchy–Euler equation and has below general solution:

$$F(r) = \begin{cases} C_1 r^{\lambda_n} + C_2 r^{-\lambda_n} & n > 0 \\ C_3 Ln(r) + C_4 & n = 0 \end{cases}. \tag{36}$$

Therefore, with substituting relations (32) and (36) on relation (29), general solution are obtained for temperature distribution in each cylindrical laminate layer. In this paper supposed that $\tau = T - T_{in}$ and implements it in heat transfer equation (27) to make boundary condition homogeneously at inside the cylinder. So below relation is obtained for temperature distribution:

$$\begin{aligned} \tau^{(i)}(r,\varphi) = {} & a_0^{(i)} Ln\left(\frac{r}{r_0}\right) \\ & + b_0^{(i)} + \sum_{n=1}^{\infty} \begin{pmatrix} a_n^{(i)} \left(\frac{r}{r_0}\right)^{n/\mu_i} + \\ b_n^{(i)} \left(\frac{r}{r_0}\right)^{-n/\mu_i} \end{pmatrix} \cos(n\varphi) \\ & + \begin{pmatrix} c_n^{(i)} \left(\frac{r}{r_0}\right)^{n/\mu_i} + \\ d_n^{(i)} \left(\frac{r}{r_0}\right)^{-n/\mu_i} \end{pmatrix} \sin(n\varphi). \end{aligned} \tag{37}$$

In order to determination of these coefficients, it needs to implement the boundary condition. Here, temperature at inside the cylinder is constant (T_{in}). Therefore τ is equal to zero at this boundary and following relations were obtained by implementing this boundary condition.

$$b_0^{(1)} = 0, \tag{38a}$$

$$a_n^{(1)} + b_n^{(1)} = 0, \tag{38b}$$

$$c_n^{(1)} + d_n^{(1)} = 0. \tag{38c}$$

Also boundary conditions of temperature continuity and heat flux continuity between layers are valid [relation (26a, b)]. By substituting the relation (37) on boundary condition (26a, b), these results are obtained:

$$a_0^{(i)} = a_0^{(i+1)}, \tag{39a}$$

$$b_0^{(i)} = b_0^{(i+1)} = 0, \tag{39b}$$

$$\begin{aligned} & a_n^{(i)} \left(\frac{r_i}{r_0}\right)^{n/\mu_i} + b_n^{(i)} \left(\frac{r_i}{r_0}\right)^{-n/\mu_i} - a_n^{(i+1)} \left(\frac{r_i}{r_0}\right)^{n/\mu_{i+1}} \\ & - b_n^{(i+1)} \left(\frac{r_i}{r_0}\right)^{-n/\mu_{i+1}} = 0, \end{aligned} \tag{39c}$$

$$\begin{aligned} & c_n^{(i)} \left(\frac{r_i}{r_0}\right)^{n/\mu_i} + d_n^{(i)} \left(\frac{r_i}{r_0}\right)^{-n/\mu_i} - c_n^{(i+1)} \left(\frac{r_i}{r_0}\right)^{n/\mu_{i+1}} \\ & - d_n^{(i+1)} \left(\frac{r_i}{r_0}\right)^{-n/\mu_{i+1}} = 0, \end{aligned} \tag{39d}$$

$$\begin{aligned} & a_n^{(i)} \left(\frac{r_i}{r_0}\right)^{n/\mu_i - 1} - b_n^{(i)} \left(\frac{r_i}{r_0}\right)^{-n/\mu_i - 1} - a_n^{(i+1)} \left(\frac{\mu_i}{\mu_{i+1}}\right) \left(\frac{r_i}{r_0}\right)^{n/\mu_{i+1} - 1} \\ & + b_n^{(i+1)} \left(\frac{\mu_i}{\mu_{i+1}}\right) \left(\frac{r_i}{r_0}\right)^{-n/\mu_{i+1} - 1} = 0, \end{aligned} \tag{39e}$$

$$\begin{aligned} & c_n^{(i)} \left(\frac{r_i}{r_0}\right)^{n/\mu_i - 1} - d_n^{(i)} \left(\frac{r_i}{r_0}\right)^{-n/\mu_i - 1} - c_n^{(i+1)} \left(\frac{\mu_i}{\mu_{i+1}}\right) \left(\frac{r_i}{r_0}\right)^{n/\mu_{i+1} - 1} \\ & + d_n^{(i+1)} \left(\frac{\mu_i}{\mu_{i+1}}\right) \left(\frac{r_i}{r_0}\right)^{-n/\mu_{i+1} - 1} = 0. \end{aligned} \tag{39f}$$

Relations (39a–f) are valid only in surfaces between each layers ($r = r_i$, $i = 1, 2, \ldots, n_{L-1}$) and There are not governed at inside and outside of the cylinder. At outside of laminate ($r = r_{nl}$) combination of convection and solar radiation was implemented as boundary condition. So by substituting relation (37) on relation (24) the following equations are achieved:

$$a_0^{(n_L)} = \frac{r_{n_L}}{k_{22} + h r_{n_L} Ln\left(\frac{r_{n_L}}{r_0}\right)} \left(\frac{q''}{\pi} + h(T_\infty - T_{in}) \right), \tag{40a}$$

$$a_n^{(n_L)}\left[h\left(\frac{r_{n_L}}{r_0}\right)^{\frac{n}{\mu_{n_L}}}+k_{22}\left(\frac{n}{r_0\mu_{n_L}}\right)\left(\frac{r_{n_L}}{r_0}\right)^{\frac{n}{\mu_{n_L}}-1}\right] + b_n^{(n_L)}\left[h\left(\frac{r_{n_L}}{r_0}\right)^{-\frac{n}{\mu_{n_L}}}-k_{22}\left(\frac{n}{r_0\mu_{n_L}}\right)\left(\frac{r_{n_L}}{r_0}\right)^{-\frac{n}{\mu_{n_L}}-1}\right] = \begin{cases} 0 \rightarrow n = \text{odd} \\ \dfrac{2q''}{\pi(1-n^2)} \rightarrow n = \text{even} \end{cases}, \tag{40b}$$

$$c_n^{(n_L)}\left[h\left(\frac{r_{n_L}}{r_0}\right)^{\frac{n}{\mu_{n_L}}}+k_{22}\left(\frac{n}{r_0\mu_{n_L}}\right)\left(\frac{r_{n_L}}{r_0}\right)^{\frac{n}{\mu_{n_L}}-1}\right] + d_n^{(n_L)}\left[h\left(\frac{r_{n_L}}{r_0}\right)^{-\frac{n}{\mu_{n_L}}}-k_{22}\left(\frac{n}{r_0\mu_{n_L}}\right)\left(\frac{r_{n_L}}{r_0}\right)^{-\frac{n}{\mu_{n_L}}-1}\right] = \begin{cases} \dfrac{q''}{2} \rightarrow n = 1 \\ 0 \rightarrow n > 1 \end{cases}, \tag{40c}$$

According to relation (38a–c)–(40a–c), coefficient a_0 and b_0 are equal in all layers and amount of $a_0^{(i)}$ is calculated from relation (40a) also the value of $b_0^{(i)}$ is equal to zero. For calculating values of $a_n^{(i)}$ and $b_n^{(i)}$ when $n > 1$, it needs to solve a five diagonal set of equations that includes Eqs. 38b, 39c, e, and 40b. Also by solving a five diagonal set of equations which includes Eqs. 38c, 39d, f and 40c the values of $c_n^{(i)}$ and $d_n^{(i)}$ will be obtained. In this research for solving these sets of equations, at first with combining these relations the set of equation has been changed to a three diagonal set of equations then it has been solved by using *LU* factorization. For determining $a_n^{(i)}$ and $b_n^{(i)}$, below three diagonal set of equations has been obtained:

$$a_n^{(1)} + b_n^{(1)} = 0, \tag{41a}$$

$$\left(1+\frac{\mu_i}{\mu_{i+1}}\right)\left(\frac{r_i}{r_0}\right)^{n/\mu_i} a_n^{(i)} + \left(\frac{\mu_i}{\mu_{i+1}}-1\right)\left(\frac{r_i}{r_0}\right)^{-n/\mu_i} b_n^{(i)} - 2\frac{\mu_i}{\mu_{i+1}}\left(\frac{r_i}{r_0}\right)^{n/\mu_{i+1}} a_n^{(i+1)} = 0, \tag{41b}$$

$$2\left(\frac{r_i}{r_0}\right)^{-n/\mu_i} b_n^{(i)} + \left(\frac{\mu_i}{\mu_{i+1}}-1\right)\left(\frac{r_i}{r_0}\right)^{n/\mu_{i+1}} a_n^{(i+1)} - \left(1+\frac{\mu_i}{\mu_{i+1}}\right)\left(\frac{r_i}{r_0}\right)^{-n/\mu_{i+1}} b_n^{(i+1)} = 0, \tag{41c}$$

$$\left[h\left(\frac{r_{n_L}}{r_0}\right)^{n/\mu_{n_L}}+k_{22}\left(\frac{n}{r_0\mu_{n_L}}\right)\left(\frac{r_{n_L}}{r_0}\right)^{n/\mu_{n_L}-1}\right] a_n^{(n_L)} + \left[h\left(\frac{r_{n_L}}{r_0}\right)^{-n/\mu_{n_L}}-k_{22}\left(\frac{n}{r_0\mu_{n_L}}\right)\left(\frac{r_{n_L}}{r_0}\right)^{-n/\mu_{n_L}-1}\right] b_n^{(n_L)} = \frac{q''\left[(-1)^{n+1}-1\right]}{\pi(n^2-1)}. \tag{41d}$$

Also with combining the five diagonal set of equations related to coefficients $c_n^{(i)}$ and $d_n^{(i)}$ below three diagonal set of equations has been obtained:

$$c_n^{(1)} + d_n^{(1)} = 0 \tag{42a}$$

$$\left(1+\frac{\mu_i}{\mu_{i+1}}\right)\left(\frac{r_i}{r_0}\right)^{n/\mu_i} c_n^{(i)} + \left(\frac{\mu_i}{\mu_{i+1}}-1\right)\left(\frac{r_i}{r_0}\right)^{-n/\mu_i} d_n^{(i)} - 2\frac{\mu_i}{\mu_{i+1}}\left(\frac{r_i}{r_0}\right)^{n/\mu_{i+1}} c_n^{(i+1)} = 0 \tag{42b}$$

$$2\left(\frac{r_i}{r_0}\right)^{-n/\mu_i} d_n^{(i)} + \left(\frac{\mu_i}{\mu_{i+1}}-1\right)\left(\frac{r_i}{r_0}\right)^{n/\mu_{i+1}} c_n^{(i+1)} - \left(1+\frac{\mu_i}{\mu_{i+1}}\right)\left(\frac{r_i}{r_0}\right)^{-n/\mu_{i+1}} d_n^{(i+1)} = 0 \tag{42c}$$

$$\left[h\left(\frac{r_{n_L}}{r_0}\right)^{n/\mu_{n_L}}+k_{22}\left(\frac{n}{r_0\mu_{n_L}}\right)\left(\frac{r_{n_L}}{r_0}\right)^{n/\mu_{n_L}-1}\right] c_n^{(n_L)} + \left[h\left(\frac{r_{n_L}}{r_0}\right)^{-n/\mu_{n_L}}-k_{22}\left(\frac{n}{r_0\mu_{n_L}}\right)\left(\frac{r_{n_L}}{r_0}\right)^{-n/\mu_{n_L}-1}\right] d_n^{(n_L)} = \begin{cases} \frac{q''}{2} & n = 1 \\ 0 & n > 1 \end{cases} \tag{42d}$$

By using *LU* factorization these results will be obtained for set of equations (41a–d) and (42a–d):

$$a_n^{(i)} = \frac{-q''\left[(-1)^{n+1}-1\right]\prod_{m=2i-1}^{2n_L-1}\gamma_m}{\pi(n^2-1)\prod_{m=2i-1}^{2n_L}\pi_m} \tag{43a}$$

$$b_n^{(i)} = \frac{q''\left[(-1)^{n+1}-1\right]\prod_{m=2i}^{2n_L-1}\gamma_m}{\pi(n^2-1)\prod_{m=2i}^{2n_L}\pi_m} \tag{43b}$$

$$c_n^{(i)} = \begin{cases} -\frac{q''}{2}\frac{\prod_{m=2i-1}^{2n_L-1}\gamma_m}{\prod_{m=2i-1}^{2n_L}\pi_m} & n = 1 \\ 0 & n > 1 \end{cases} \tag{43c}$$

$$d_n^{(i)} = \begin{cases} \frac{q''}{2}\frac{\prod_{m=2i}^{2n_L-1}\gamma_m}{\prod_{m=2i}^{2n_L}\pi_m} & n = 1 \\ 0 & n > 1 \end{cases} \tag{43d}$$

In relation (43a–d) coefficients γ_i and π_i will be calculated as below:

$$\gamma_1 = 1 \tag{44a}$$

$$\gamma_{2i} = -2\frac{\mu_i}{\mu_{i+1}}\left(\frac{r_i}{r_0}\right)^{n/\mu_{i+1}} \tag{44b}$$

$$\gamma_{2i+1} = -\left(1+\frac{\mu_i}{\mu_{i+1}}\right)\left(\frac{r_i}{r_0}\right)^{-n/\mu_{i+1}} \tag{44c}$$

$$\pi_1 = 1 \tag{44d}$$

$$\pi_{i+1} = \beta_{i+1} - \frac{\chi_i \gamma_i}{\pi_i} \tag{44e}$$

In relation (44e) χ_i and β_i will be calculated as below:

$$\chi_{2i-1} = \left(1 + \frac{\mu_i}{\mu_{i+1}}\right)\left(\frac{r_i}{r_0}\right)^{n/\mu_i} \tag{45a}$$

$$\chi_{2i} = 2\left(\frac{r_i}{r_0}\right)^{-n/\mu_i} \tag{45b}$$

$$\chi_{2n_L-1} = \left[h\left(\frac{r_{n_L}}{r_0}\right)^{n/\mu_{n_L}} + k_{22}\left(\frac{n}{r_0\mu_{n_L}}\right)\left(\frac{r_{n_L}}{r_0}\right)^{n/\mu_{n_L}-1}\right] \tag{45c}$$

$$\beta_1 = 1 \tag{45d}$$

$$\beta_{2i} = \left(\frac{\mu_i}{\mu_{i+1}} - 1\right)\left(\frac{r_i}{r_0}\right)^{-n/\mu_i} \tag{45e}$$

$$\beta_{2i+1} = \left(\frac{\mu_i}{\mu_{i+1}} - 1\right)\left(\frac{r_i}{r_0}\right)^{n/\mu_{i+1}} \tag{45f}$$

$$\beta_{2n_L} = \left[h\left(\frac{r_{n_L}}{r_0}\right)^{-n/\mu_{n_L}} - k_{22}\left(\frac{n}{r_0\mu_{n_L}}\right)\left(\frac{r_{n_L}}{r_0}\right)^{-n/\mu_{n_L}-1}\right] \tag{45g}$$

5 Results and discussion

In this section, analytical solution results for steady-state conductive heat transfer in cylindrical laminate under specific boundary conditions that defined in Sect. 3 are described. In this paper, for investigation of heat transfer in composite materials, effects of fibers angle in heat transfer in one-layer laminate was studied, also the temperature distribution in multi layers laminates with different fibers arrangement was investigated.

Composite material considered in this section is 25% epoxy and 75% graphite fibers (graphite/epoxy). The reason of selecting this composite is significant difference between conductive heat transfer coefficient in fibers and in matrix materials (because Graphite is a conductive material and epoxy is heat insulator). High difference between conductive coefficients of fibers and matrix material leads to 12.76 times larger than conductive coefficient in direction of fibers compared with direction perpendicular to the fibers, and heat analysis in this composite can help us to understand heat transfer in orthotropic materials. There are some lists of physical properties of the fibers in Table 1 and matrix material and composite material properties in Table 2. Initially, to better understanding of heat transfer in composite materials, it is observed a one-layer composite laminate (one-layer or multilayer with equal fiber angle) with geometry and boundary conditions according to information presented in Table 3.

Table 1 Properties of graphite fiber and epoxy matrix [32]

Matrix material	Epoxy
Fibers material	Graphite
Conductive coefficient of matrix (W/m K)	0.19
Conductive coefficient of fibers (W/m K)	14.74
Heat capacity of matrix (J/kg K)	1613
Heat capacity of fibers (J/kg K)	709

Table 2 Properties of Graphite/Epoxy composite material [32]

k in parallel direction of fibers (W/m K)	11.1
k in perpendicular direction of fibers (W/m K)	0.87
Volumetric percentage of fibers	75
Melting point (K)	450
Heat capacity (J/kg K)	935
Density (kg/m^3)	1400

Table 3 Geometry and boundary conditions

Inner diameter (cm)	30
Outer diameter (cm)	42
Solar radiation flux (W/m^2)	700
Free convection coefficient (W/m^{2}K)	20
Inner temperature of cylinder (K)	320
Temperature of environment (K)	300
Angle of fibers (degree)	90

Figure 5 shows the maximum temperature variations in different value of Fourier series terms for a single layer laminate with 90° fibers' angle. According to this figure, the Fourier series becomes convergent quickly in 200th terms of these series and temperature variation is reduced quickly. Therefore, it seems that to make convergence conditions, just calculating until 200th terms of Fourier series is sufficient. Figure 6 shows temperature distribution in the single layer laminate since the fibers angle are 90° and 0° with different radiation heat fluxes. Since in the case

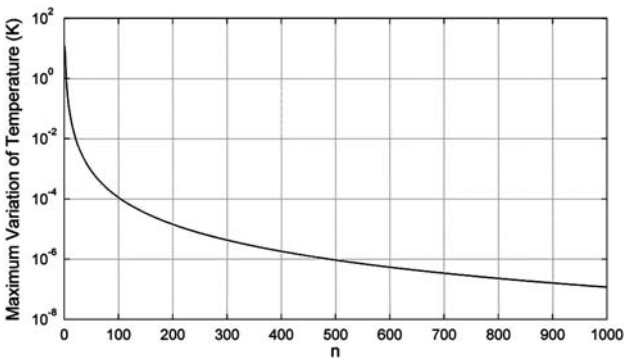

Fig. 5 Maximum temperature variations in terms of different Fourier series terms in a single layer laminate ($\varphi = 90°$)

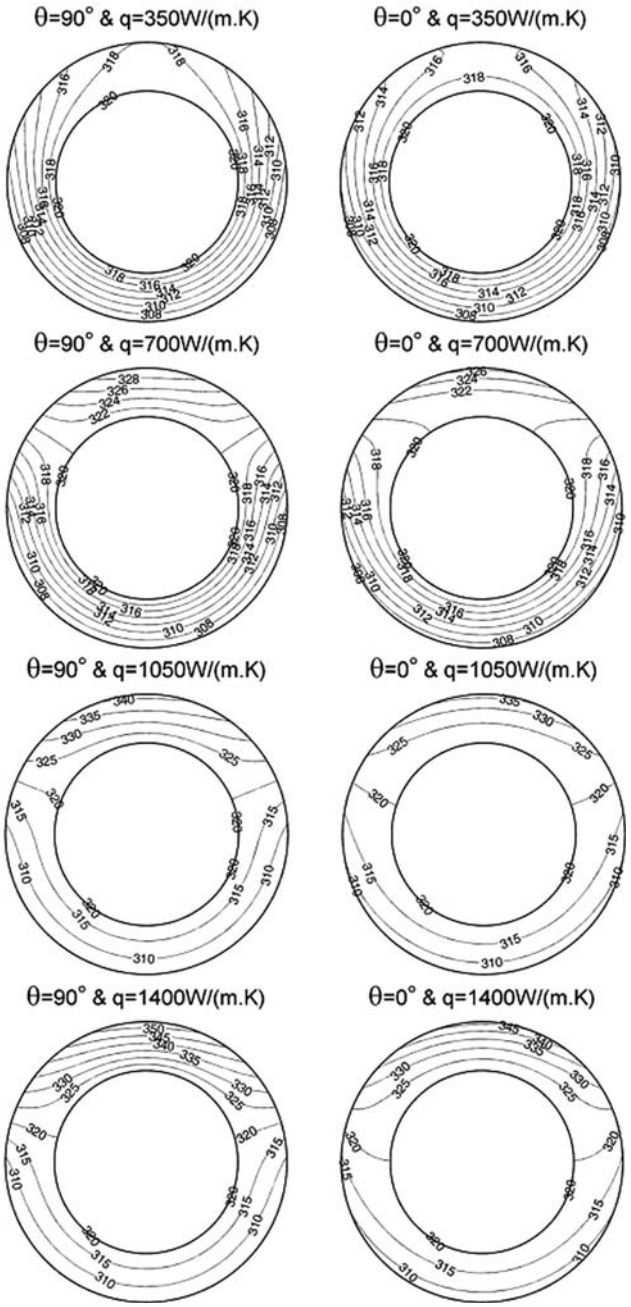

Fig. 6 Temperature distribution in a single layer laminate in different fibers' angle and different radiation fluxes

of fibers' angle is 90°, the direction of fibers is in z axis, therefore heat transfer in laminate is similar to isotropic material with conductivity coefficient of k_{22}. According to this figure, in case of $q'' = 350$ W/mK, the maximum temperature is in inside the wall of cylinder and it is equal to 320°K because of weakness of the radiation flux. But in higher radiation flux; more than $q'' = 407$ W/mK, the pattern of temperature distribution changes and maximum temperature will be shifted to outside wall of cylinder, also for each radiation flux, temperature gradient when angle of fibers is zero is less than case that fibers' angle is 90°. It seems that heat conduction is better in fibers that its angle is equal to zero and maximum of temperature is the least in these fibers' angle. Because in these laminates conductive coefficient in direction of r is equal to k_{22} and in direction of φ is equal to k_{11}; unlike in laminate that fibers' angle is 90° that cross section of cylinder is an isotropic material and its conductive coefficient is k_{22} ($k_{rr} = k_{\varphi\varphi} = k_{22}$). According to this fact, in graphite/epoxy composite k_{11} is larger than k_{22}, so effective conductive coefficient in laminate with zero fibers' angle is larger than 90° fibers' angle and therefore heat conduction is better in this state.

In Fig. 7, distribution of coefficients of heat transfer equation (μ) is shown based on fibers' angle [note to Eq. (28)]. According to this figure, this coefficient symmetrical against angle 90° and its period is 180° and maximum amount of this curve is located on 90°. According to Eq. (27), decreasing of μ, helps to reduce temperature gradient effect in direction of φ. In this research to study the effect of fibers' angle on temperature of laminate relative temperature parameter has been used $[(T - T_{in})/(T_\infty - T_{in})]$.

Figure 8 shows effect of fibers' angle on maximum of relative temperature of single layer laminate under

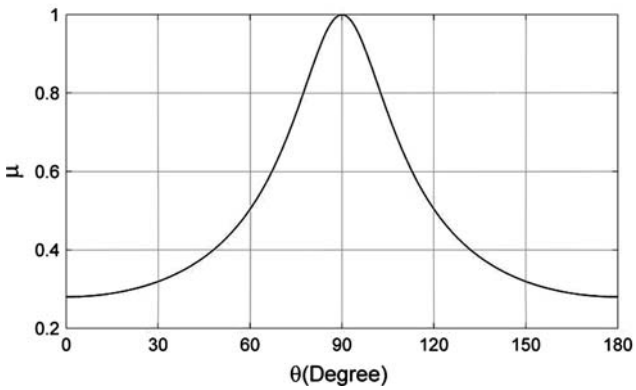

Fig. 7 Diagram of coefficient μ in terms of fibers' angle (θ)

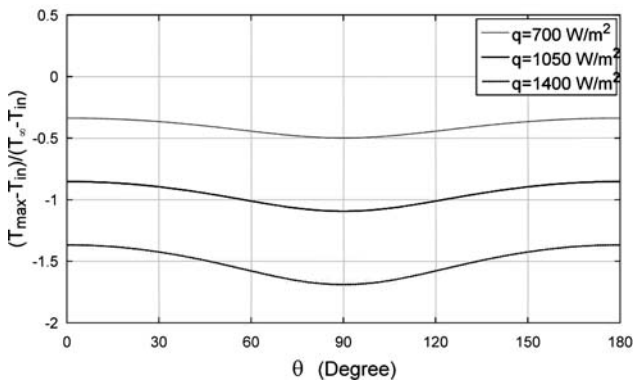

Fig. 8 Maximum of relative temperature distribution in terms of fibers' angle (θ) under different radiation fluxes

different radiation heat fluxes. In this condition maximum of relative temperature is negative because here supposed that the ambient temperature is less than the inside temperature of cylinder ($T_\infty - T_{in} < 0$). According to Fig. 7 when fibers' angle approaches to 90° then the value of μ will be increased and conductive coefficient in direction of φ will be decreased, thus temperature gradient will be increased in laminate and this fact causes the growth of maximum temperature of laminate. For heat fluxes which are 700, 1,050 and 1,400, changing of fibers' angle from 0° to 90° causes the increasing of maximum temperature in laminate by 3.2188, 4.8283 and 6.4377 K, respectively. It is noticeable that for heat fluxes that are smaller than 407 W/m^2, pattern of temperature distribution changes and maximum temperature is at inner wall of cylinder and it is equal to 320 K (see Fig. 6). Hence, for heat fluxes which are smaller than 407 W/m^2, the amount of maximum of relative temperature is zero.

Figure 9 shows mean amount of relative temperature in laminate in terms of fibers' angle and for two different heat fluxes: 350 and 1,400 W/m^2. According to Fig. 6, pattern of temperature distribution for these two heat fluxes are different, so when heat flux is 350 W/m^2 maximum temperature is at inner wall of cylinder but while heat flux is 1,400 W/m^2, maximum temperature is at outer wall of cylinder. Thus for these reason, the mean amount of relative temperature is positive for 350 W/m^2 and is negative when heat flux is 1400 W/m^2. Variation of fibers' angle from 0° to 90° decrease the mean amount of temperature in laminate to 0.0051 and 0.0204 K, respectively.

In other arrangements of fibers in multi layers laminates which have been made of graphite/epoxy, temperature distribution is similar to a state between a single layer laminate that fibers' angle is 0° and a single layer laminate that fibers' angle is 90°. According to Fig. 6, when fibers' angle is 0° there is the best heat conduction in laminate and on the contrary, for 90° there is the worst heat conduction.

Figure 10 shows temperature distribution in eight-layers cylindrical laminate which is quasi-isotropic under

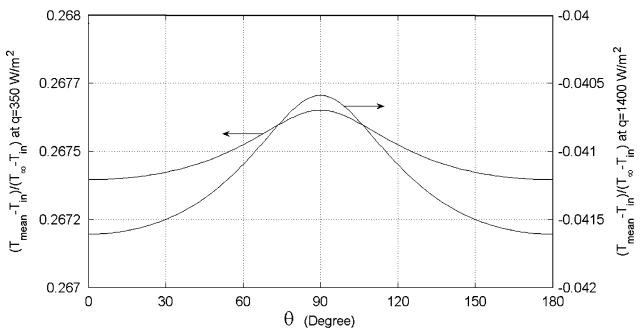

Fig. 9 Average of relative temperature distribution in terms of fibers' angle (θ) under different radiation fluxes

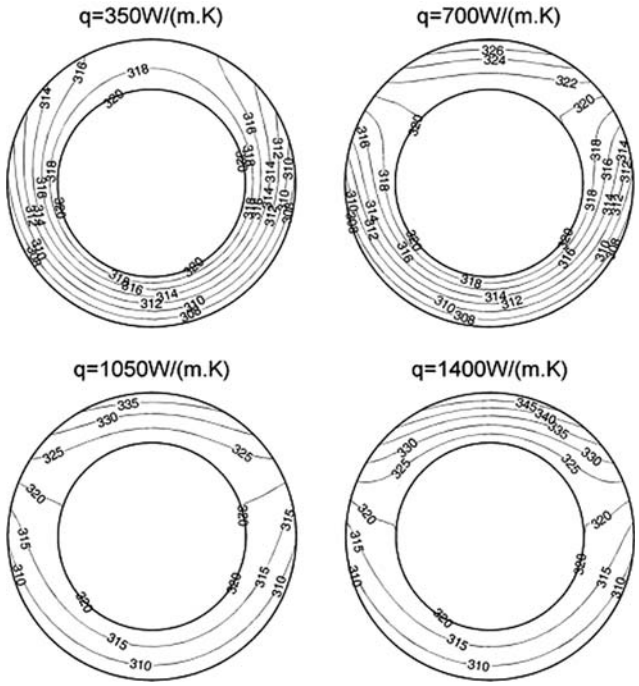

Fig. 10 Temperature distribution in quasi-isotropic laminate under different radiation fluxes

different heat fluxes. In this condition all of specifications of laminate and its heat conditions are according to Table 3. In this case, thickness of each layer is 1 mm and arrangement of fibers' angle in different laminas is [0°, 45°, 90°, 135°, 180°, 225°, 270°, 315°]. By comparing between Fig. 10 and Fig. 6, it is clear that temperature distribution in this laminate is a state between single layer laminate which fibers' angle is 0° and 90°. Also, when heat fluxes are 350, 700, 1,050 and 1,400 W/m.K; therefore, the maximum temperatures in quasi-isotropic laminate are 320.00, 328.26, 339.32 and 350.38 K, respectively. Also mean temperatures are 314.65, 316.69, 318.73 and 320.77 K, respectively. Figures 11 and 12 show terms of Fourier series of temperature distribution [according to relation

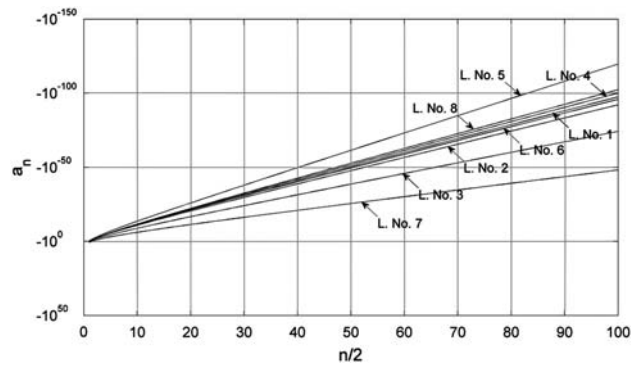

Fig. 11 Fourier series terms (an) distribution in terms of $n/2$ in a quasi-isotropic laminate

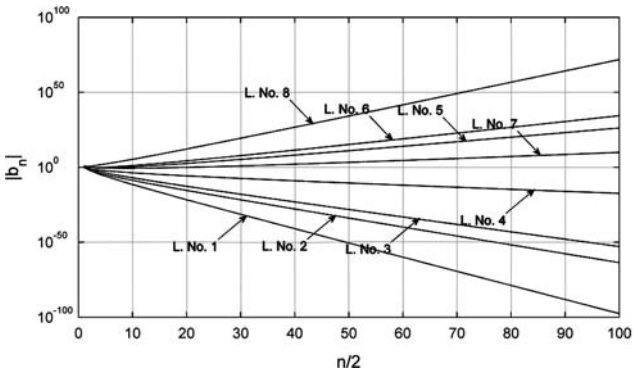

Fig. 12 Fourier series terms (bn) distribution in terms of $n/2$ in a quasi-isotropic laminate

(37)] for quasi-isotropic laminate. Because of the odd terms of this series are zero, so its diagram has been shown in terms of $n/2$. The amount of a_n is positive but b_n is negative in fourth, fifth and eighth layer and it is positive in other layers. According to this figure, a_n are very small numbers that will be decreased sharply by increasing the amount of n. Because a_n is a coefficient that multiply to $(r/r_0)^{n/\mu}$ terms of Fourier series and amount of these terms are large, so it is necessary that amount of a_n must be very small to converge these series. Also c_n is a positive coefficient and d_n is negative, which are valuable only for $n = 1$ [see relations (43c) and (43d)].

6 Conclusions

In this present paper, tensor and heat transfer equations in composite laminate materials are introduced and the method of determining conduction coefficients for these materials are discussed, then an exact analytical solution for heat transfer in 2-dimensional cylindrical composite laminate was presented. This solution is applicable directly in cylindrical composite pipes and reservoirs. One of the most significant results is the effect of the arrangement of fibers' angle in laminate on temperature distribution.

Therefore in any engineering application, regarding to design objectives, the appropriate heat distribution can be obtained through selection of composite material and direction of fibers in each layer. For example, if the goal is reducing thermal stress in laminate, the temperature gradient can be reduced with appropriate selection of direction of fibers in each layer. In this research heat transfer in graphite/epoxy composite laminate has been investigated. In this laminate if fibers' angle was 0°, is in the best condition and when fibers' angle is 90°, heat conduction is weak. In other arrangement of fibers, the temperature distribution is in a state between two previous states. Because in graphite/epoxy composite conductive coefficient is large in direction along of fibers compare to perpendicular direction of fibers. This result is valid for other composites when $k_{11} > k_{22}$ and in some composites that $k_{11} > k_{22}$ is reverse.

References

1. Wooster WA (1957) A textbook in crystal physics. Cambridge University Press, London, p 455
2. Nye JF (1957) Physical properties of crystals. Clarendon Press, London, p 309
3. Özisik MN (1993) Heat conduction. Wiley, New York
4. Chang YP, Tsou CH (1977) Heat conduction in an anisotropic medium homogeneous in cylindrical coordinates, steady-state. J Heat Transfer 99C:132–134
5. Chang YP, Tsou CH (1977) Heat conduction in an anisotropic medium homogeneous in cylindrical coordinates, unsteady state. J Heat Transfer 99C:41–47
6. Özisik MN, Shouman SM (1980) Transient heat conduction in an anisotropic medium in cylindrical coordinates. J Franklin Inst 309:457–472
7. Mulholland GP (1974) Diffusion through laminated orthotropic cylinders, Tokyo. In: Proceeding of the 5th international heat transfer conference, pp 250–254
8. Noor AK, Burton WS (1990) Center for computational structures technology, University of Virginia, NASA Langley Research Center, and Hampton, VA 23665
9. Iyengar V (1995) Transient thermal conduction in rectangular fiber reinforced composite laminates. Adv Compos Mater 4(4):327–342
10. Argyris J, Tenek L, Oberg F (1995) A multilayer composite triangular element for steady-state conduction/convection/radiation heat transfer in complex shells. Comput Methods Appl Mech Eng 120:271–301
11. Sunao S, Takashi I (1999) Numerical analysis of heat conduction effect corresponding to infrared stress measurements in multilamina CFRP plates. Adv Compos Mater 8(3):269–279
12. Tarn JQ (2001) Exact solutions for functionally graded anisotropic cylinders subjected to thermal and mechanical loads. Int J Solids Struct 38:8189–8206
13. Tarn JQ (2002) state space formalism for anisotropic elasticity. Part II: cylindrical anisotropy. Int J Solids Struct 39:5157–5172
14. Tarn JQ, Wang YM (2003) Heat conduction in a cylindrically anisotropic tube of a functionally graded material. Chin J Mech 19:365–372
15. Tarn JQ, Wang YM (2004) End effects of heat conduction in circular cylinders of functionally graded materials and laminated composites. Inter J Heat Mass Transfer 47:5741–5747
16. Golovchan VT, Artemenko AG (2004) heat conduction of orthogonally reinforced composite material. J Eng Phys Thermo Phys 51(2):944–949
17. Shi-qiang D, Jia-chan L (2005) Homogenized equations for steady heat conduction in composite materials with dilutely-distributed impurities. J Appl Math Mech 4(2):167–173
18. Guo Z-S et al (2004) Temperature distribution of thick thermo set composites. J Model Simul Mater Sci Eng 12:443–452
19. Greengard L, Lee JY (2006) Electrostatics and heat conduction in high contrast composite materials. J Comput Phys 21(1):64–76
20. Lu X, Tervola P, Viljanen M (2006) Transient Analytical Solution to Heat Conduction in Composite Circular Cylinder. Int J Heat Mass Transf 49:341–348

21. Chatterjee J, Henry DP, Ma F, Banerjee PK (2008) An efficient BEM formulation for 3-dimensional steady-state heat conduction analysis of composites. Int J Heat Mass Transf 51:1439–1452
22. Yvonnet J, He QC, Toulemonde C (2009) Numerical modeling of the effective conductivities of composites with arbitrarily shaped inclusions and highly conducting interface, Composites Science and Technology (in press)
23. Sadowski T, Ataya S, Nakonieczny K (2008) Thermal analysis of layered FGM cylindrical plates subjected to sudden cooling process at one side–Comparison of two applied methods, for problem solution, Computational Materials Science, in press
24. Chiu CH, Cheng CC, Hwan CL, Tsai KH (2006) Cylindrical orthotropic thermal conductivity of spiral woven composites. Part II: a mathematical model for their effective transverse thermal conductivity. Polym Polym Compos 14(4):349–364
25. Chiu CH, Hwan CL, Cheng CC, Tsai KH (2007) Cylindrical orthotropic thermal conductivity of spiral woven composites. Part III: an estimation of their thermal properties. Polym Polym Compos 15(3):167–182
26. Fung YC (1965) Foundation of solid mechanics. Prentice-Hall, Englewood Cliffs
27. Powers JM (2004) On the necessity of positive semi-definite conductivity and Onsager reciprocity in modeling heat conduction in anisotropic media. J Heat Transf Trans Asme 126(5):670–675
28. Herakovich CT (1998) Mechanics of fibrous composites. Wiley, New York
29. Halpin JC (1992) Primer on composite materials analysis. CRC Press, Boca Raton
30. Carslaw HS, Jaeger JC (1971) Conduction of heat in solids. Oxford University Press, London
31. Arpaci VS (1966) Conduction Heat Transfer. Addison-Wesley Publishing Company, USA
32. Touloukian YS, Ho CY (1972) Thermophysical properties of matter, plenum press, vol 2. Thermal Conductivity of Nonmetallic Solids, New York, p 740